

Light Heavy MSSM Higgs Bosons at Large $\tan\beta$

J. Ellis¹, S. Heinemeyer², K.A. Olive³ and G. Weiglein⁴

¹*TH Division, Physics Department, CERN, Geneva, Switzerland*

²*Instituto de Fisica de Cantabria (CSIC-UC), Santander, Spain*

³*William I. Fine Theoretical Physics Institute,
University of Minnesota, Minneapolis, MN 55455, USA*

⁴*IPPP, University of Durham, Durham DH1 3LE, UK*

Abstract

The region of MSSM Higgs parameter space currently excluded by the CDF Collaboration, based on an analysis of $\sim 1 \text{ fb}^{-1}$ of integrated luminosity, is less than the expected sensitivity. We analyze the potential implications of the persistence of this discrepancy within the MSSM, assuming that the soft supersymmetry-breaking contributions to scalar masses are universal, apart from those to the Higgs masses (the NUHM model). We find that a light heavy MSSM Higgs signal in the unexcluded part of the sensitive region could indeed be accommodated in this simple model, even after taking into account other constraints from cold dark matter, electroweak precision observables and B physics observables. In this case the NUHM suggests that supersymmetric signatures should also be detectable in the near future in some other measurements such as $\text{BR}(B_s \rightarrow \mu^+ \mu^-)$, $\text{BR}(b \rightarrow s\gamma)$ and $(g-2)_\mu$, and M_h would have to be very close to the LEP exclusion limit. In addition, the dark matter candidate associated with this model should be on the verge of detection in direct detection experiments.

The searches for the bosons appearing in its extended Higgs sector are among the most promising ways to search for evidence of supersymmetry (SUSY) at the Tevatron collider. The CDF and D0 Collaborations have already established important limits on the (heavier) MSSM Higgs bosons, particularly at large $\tan\beta$ [1–5]. Recently the CDF Collaboration, investigating the channel

$$p\bar{p} \rightarrow \phi \rightarrow \tau^+\tau^-, \quad (\phi = h, H, A), \quad (1)$$

has been unable to improve these limits to the extent of the sensitivity expected with the analyzed integrated luminosity of $\sim 1 \text{ fb}^{-1}$ [4], whereas there is no indication of any similar effect in D0 data [5].¹ Time will tell whether the CDF effect persists. Within the MSSM the channel (1) is enhanced as compared to the corresponding SM process by roughly a factor of $\tan^2\beta / ((1 + \Delta_b)^2 + 9)$ [7], where $\tan\beta$ is the ratio of the two vacuum expectation values, and Δ_b includes loop corrections to the $\phi b\bar{b}$ vertex (see Ref. [7] for details) and is subdominant for the $\tau^+\tau^-$ final state. Correspondingly, the unexpected weakness of the CDF exclusion might be explicable within the MSSM if $M_A \approx 160 \text{ GeV}$ and $\tan\beta \gtrsim 45$ and, doubtless, also within other theoretical frameworks.

In this paper we investigate whether light heavy Higgs bosons just beyond the region currently excluded by CDF could be accommodated within GUT-inspired MSSM scenarios, and what the possible consequences would be. We consider the constraints imposed by other measurements, such as the limits on $\text{BR}(B_s \rightarrow \mu^+\mu^-)$, $\text{BR}(b \rightarrow s\gamma)$, $(g - 2)_\mu$ and M_h , assuming that R parity is conserved and that the lightest neutralino $\tilde{\chi}_1^0$ constitutes the astrophysical dark matter [8]. Whereas we find no solution within the constrained MSSM (CMSSM), in which all soft SUSY-breaking contributions to scalar masses are assumed to unify at the GUT scale, we find that all the constraints may be satisfied in the case that universality at the GUT scale is relaxed for the scalar Higgs mass parameters (the NUHM model [9–11]). However, we point out that any interpretation of the CDF effect within the NUHM would be tightly constrained by the other measurements. Specifically, the constraints are so tight that one or more of these measurements should display a discrepancy with the SM, either now or in the near future.

The essence of the argument is as follows. The absence of exclusion by CDF, compared to their expected sensitivity, as mentioned above, would correspond to $M_A(\approx M_H) \sim 160 \text{ GeV}$, and a value of $\tan\beta \sim 45$ or greater. Since the H/A contribution to $\text{BR}(B_s \rightarrow \mu^+\mu^-) \sim$

¹The same analysis shows a deficit of $Z \rightarrow \tau^+\tau^-$ events compared to the Standard Model (SM) expectation. Changing the luminosity by one σ to accommodate this ‘deficit’ would raise the observed rate of $\tau^+\tau^-$ final states around $M_A = 160 \text{ GeV}$ slightly above the expected rate (by somewhat less than one σ) [6].

$\tan^6 \beta$, values of $\tan \beta \gtrsim 45$ are already excluded for this value of M_A for substantial portions of the NUHM parameter space, depending largely on the values of $m_{1/2}$ and m_0 . The parameter space is so constrained that, in areas which are still allowed, we expect that a SUSY signal should appear very soon, as we show below. We assume R -parity conservation, and restrict our attention to the NUHM with values of the relic CDM density Ω_{CDM} that fall within the range favoured by WMAP and other astrophysical and cosmological observations. This restriction imposes important constraints on $m_{1/2}$ and μ , the values of m_0 and A_0 being less essential. As for $\text{BR}(b \rightarrow s\gamma)$, it is well known that the world average experimental value currently agrees well with the SM [12]. In the MSSM, there are two important contributions with opposite signs, due to H^\pm and chargino exchanges, respectively. In order for the net MSSM contribution to be unnoticeable so far, the H^\pm and chargino exchanges must cancel to a great extent, imposing a relation between the H^\pm and chargino masses. Since the H^\pm mass is very similar to the H, A masses, this yields a preferred range of relatively small values of the chargino mass and hence the soft supersymmetry-breaking gaugino mass $m_{1/2}$, favouring in turn a non-negligible contribution to $(g-2)_\mu$. The combination of a preferred value for $m_{1/2}$ and the WMAP constraint then limits the possible range of μ . The preference for relatively light sparticles (see also Ref. [13]) translates into a relatively small value for M_h , and compatibility between the LEP limit on M_h [14, 15] and the upper limit on $\text{BR}(B_s \rightarrow \mu^+ \mu^-)$ [16, 17] selects a limited range of A_0 .

In preparation for our survey of the NUHM parameter space, we first recall that in the CMSSM, the electroweak vacuum conditions determine $|\mu|$ and M_A in terms of $\tan \beta$ and the input soft supersymmetry-breaking parameters. In the NUHM, these are the scalar mass m_0 (which is assumed to be universal, except for the Higgs multiplets)², the gaugino mass $m_{1/2}$, the trilinear coupling A_0 and the degrees of non-universality of the soft supersymmetry-breaking contributions to the masses of the two Higgs doublets. In our analysis, we invert the electroweak vacuum conditions, treating $|\mu|$ and M_A as free parameters and adjusting the non-universal Higgs mass inputs accordingly. In the cases of interest this difference in the scalar masses at the GUT scale is no more than 50% for low values of m_0 , and of order 10% for higher values of m_0 . The values $M_A = 160$ GeV and $\tan \beta \geq 45$ are chosen to match the excess of signal-like events observed in CDF, and we assume that $\mu > 0$ so as to avoid severe problems with $(g-2)_\mu$ and $\text{BR}(b \rightarrow s\gamma)$. Hence our four free parameters are $m_{1/2}, m_0, A_0$ and $\mu > 0$. However, these are tightly constrained by other phenomenological limits, as we now discuss.

Since we assume that R parity is conserved, and that the lightest neutralino $\tilde{\chi}_1^0$ constitutes

²We discuss later the implications of relaxing this assumption.

the astrophysical dark matter [18], we impose the requirement that the relic neutralino density falls within the range allowed by WMAP and other observations: $0.085 < \Omega_{\text{CDM}} h^2 < 0.119$ [8]. As we see later, requiring the relic density to fall within this narrow range effectively reduces the dimensionality of the NUHM parameter space. In order to apply the constraints on the NUHM parameter space that are provided by $\text{BR}(b \rightarrow s\gamma)$, $\text{BR}(B_s \rightarrow \mu^+\mu^-)$, $(g-2)_\mu$ and M_h , we use the following experimental values and theory evaluations (for more details, specifics on error treatments and an extended list of references see Ref. [19]): $\text{BR}(b \rightarrow s\gamma)_{\text{exp}} = (3.55 \pm 0.24) \times 10^{-4}$ [12], where the theory evaluation is based on Refs. [20, 21]; $\text{BR}(B_s \rightarrow \mu^+\mu^-)_{\text{exp}} < 10^{-7}$ [16, 17], where details about the theory evaluation can be found in Ref. [22]; $(g-2)_\mu, \text{exp-SM} = (27.5 \pm 8.4) \times 10^{-10}$ [23] (for a discussion and references to other determinations, see Ref. [19]), and $M_h > 114.4$ GeV [14, 15], where the theory calculations have been performed with **FeynHiggs** [24]. These observables impose important constraints, as we now show ³.

We consider first the $(m_{1/2}, m_0)$ plane shown in panel a) of Fig. 1, which has $\tan \beta = 45$, $\mu = 370$ GeV and $A_0 = -1800$ GeV, as well as $M_A = 160$ GeV.⁴ The dark (brown) shaded region at low m_0 is forbidden, because there the LSP would be the lighter stau. The WMAP cold dark matter constraint is satisfied only within the lighter (turquoise) shaded region. To the left of this region, the relic density is too small, due to s -channel annihilation through the Higgs pseudoscalar A . As $m_{1/2}$ increases away from the pole, the relic density increases toward the WMAP range. However, as $m_{1/2}$ is increased, the neutralino acquires a larger Higgsino component and annihilations to pairs of W and Z bosons become enhanced. To the right of this transition region, the relic density again lies below the WMAP preferred value. The shaded region here is therefore an overlap of the funnel and transition regions discussed in Ref. [10].

The $\text{BR}(B_s \rightarrow \mu^+\mu^-)$ constraint is satisfied between the outer black dash-dotted lines, labelled 10^{-7} , representing the current limit on that branching ratio⁵. Also shown are the contours where the branching ratio is 2×10^{-8} , close to the sensitivity likely to be attainable soon by CDF and D0. Between these two contours, there is a strong cancellation between the flavor-violating contributions arising from the Higgs and chargino couplings at the one-loop level and the Wilson coefficient counterterms contributing to $\text{BR}(B_s \rightarrow \mu^+\mu^-)$.

³Consequences for other observables such as $\text{BR}(B_u \rightarrow \tau\nu_\tau)$ and the W -boson mass are discussed further below.

⁴Here and elsewhere, we assume $m_t = 171.4$ GeV and $m_b(m_b) = 4.25$ GeV, but our results are insensitive to the exact values of m_t and m_b , and take into account their current uncertainties, $\delta m_t = 1.8$ GeV and $\delta m_b(m_b) = 0.11$ GeV.

⁵A slightly more stringent upper limit of 0.93×10^{-7} at the 95% C.L. has been announced more recently by the D0 Collaboration [25]. However, applying this limit would have only a minor impact on our analysis.

The dash-dotted (red) line shows the contour corresponding to $M_h = 114$ GeV, and only the region to the right of this line is compatible with the constraint imposed by M_h (it should be kept in mind that there is still a ~ 3 GeV uncertainty in the prediction of M_h [24]). Also shown in pink shading is the region favoured by $(g - 2)_\mu$ at the two- σ level. The one- and two- σ contours for $(g - 2)_\mu$ are shown as elliptical dashed and solid black contours, respectively. The region which is compatible with the WMAP relic density and M_h , and is also within the two- σ $(g - 2)_\mu$ experimental bound, has $\text{BR}(B_s \rightarrow \mu^+ \mu^-) > 2 \times 10^{-8}$. The measured value of $\text{BR}(b \rightarrow s\gamma)$ is in agreement with the theory prediction only to the left of the solid (green) region. We see, in the space between the M_h and $b \rightarrow s\gamma$ exclusions, a slightly diagonal allowed strip of width $\lesssim 200$ GeV in $m_{1/2}$.

We see that there is a narrow wedge of allowed parameter space in Fig. 1(a), which has $m_{1/2} \sim 600$ GeV and $m_0 \sim 700$ to 1100 GeV. The $\text{BR}(b \rightarrow s\gamma)$ constraint is satisfied easily throughout this region, and $(g - 2)_\mu$ cuts off the top of the wedge, which would otherwise have extended to $m_0 \gg 1500$ GeV. Within the allowed wedge, M_h is very close to the LEP lower limit, and $\text{BR}(B_s \rightarrow \mu^+ \mu^-) > 2 \times 10^{-8}$. If M_A were much smaller (< 130 GeV), there would be no wedge consistent simultaneously with the Ω_{CDM} , M_h and $\text{BR}(B_s \rightarrow \mu^+ \mu^-)$ constraints (the M_h bound, however, could then be relaxed due to a weaker hZZ coupling). At higher values of $\tan \beta$, the allowed region drifts up to higher values of m_0 , as is shown in Fig. 1(c) for $\tan \beta = 55$ for the same input values of μ , M_A , and A_0 .

We have also considered the potential impact of direct searches for supersymmetric cold dark matter in the NUHM. As has been pointed out previously [26], these searches are potentially important at small M_A and large $\tan \beta$, as required in the scenario discussed here (see also Ref. [27]). However, the interpretation of the search limits is less precise than for the other constraints, for two reasons. One is the local density of supersymmetric cold dark matter, which is usually estimated as $0.3 \text{ GeV}/\text{cm}^3$. This estimate is subject to a systematic uncertainty that is itself uncertain, but might be $\sim 50\%$ or so. The second significant uncertainty is in the hadronic scattering matrix element of the local operator generated by the short-distance supersymmetric physics. The dominant contribution to the scattering is spin-independent, and given by the matrix elements in the nucleons of the scalar quark densities $\bar{q}q$: $q = u, d, s$. These may be determined from the octet matrix element σ_0 , which is estimated to be 36 ± 7 MeV, and the π -N scattering matrix element $\Sigma_{\pi N} = 45 \pm 8$ MeV. These give a range $y \equiv 2\langle N|\bar{s}s|N\rangle/\langle N|(\bar{u}u + \bar{d}d)|N\rangle = 0.2 \pm 0.2$ [28]. Generally speaking, the dark-matter scattering cross section increases with y .

Given the matrix element uncertainties summarized above, we show in Fig. 1a) the 1- σ lower limit on the calculated value of the elastic cross section as compared to the CDMS

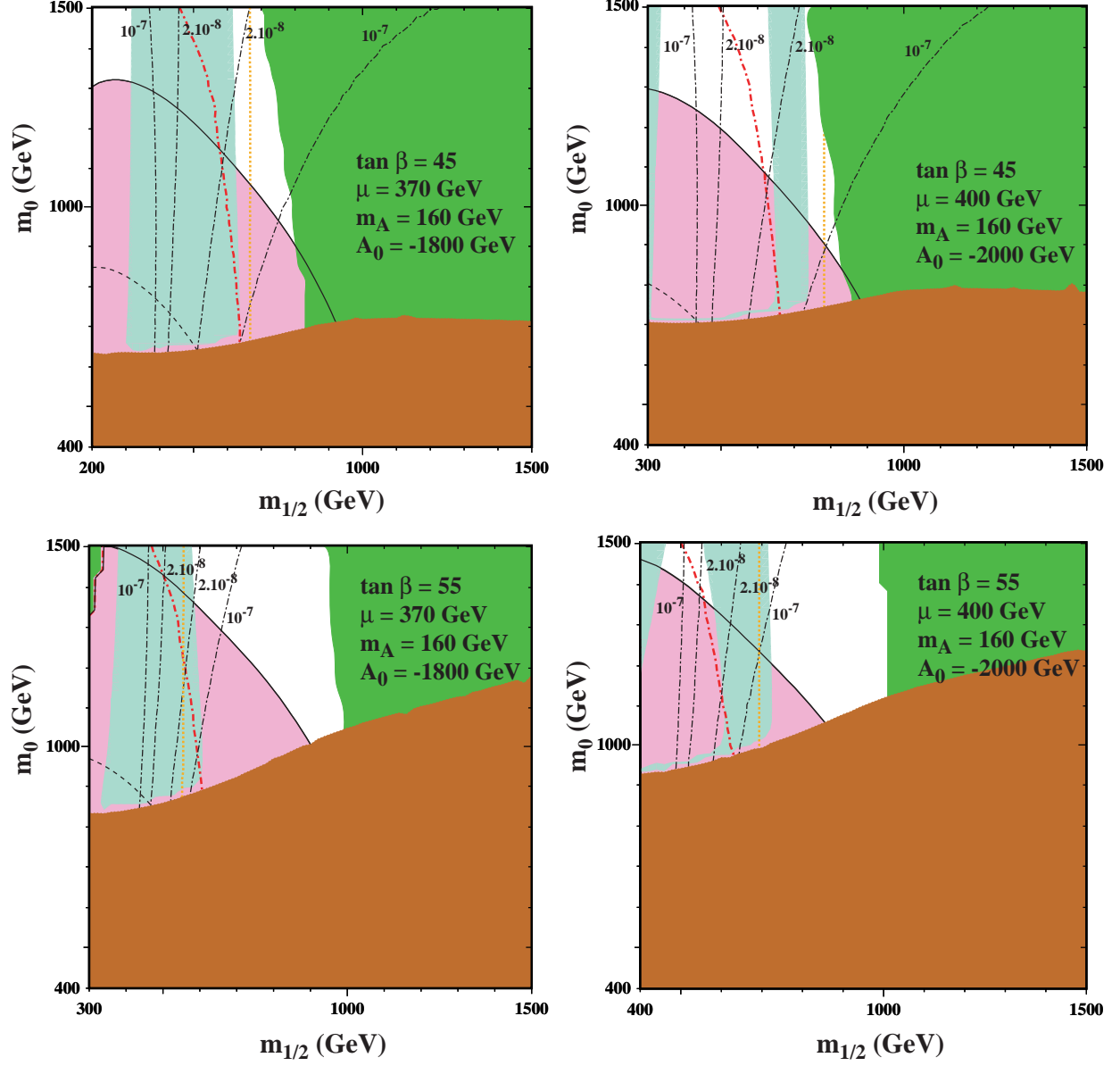


Figure 1: The NUHM parameter space as a function of $m_{1/2}$ and m_0 for $\mu = 370(400)$ GeV and $A_0 = -1800(-2000)$ GeV in the left (right) plots. We fix $M_A = 160$ GeV, $\tan \beta = 45(55)$, $m_t = 171.4$ GeV and $m_b = 4.25$ GeV in the upper (lower) plots. For the description of the various lines and shaded areas, see the text.

upper limit [29]. In the portion of the plane to the left of the (orange) dotted line, the lower limit on the calculated spin-independent elastic cross section is smaller than the CDMS upper bound, assuming the canonical local density. Whilst we have assumed $\Sigma_{\pi N} = 45$ MeV, the calculated lower limit effectively assumes zero strangeness contribution to the proton mass, i.e., $y = 0$. In the region of interest, the lower limit on the calculated cross section is about 80% of the CDMS upper bound, whereas with a strangeness contribution of $y = 0.2$, the cross section would exceed the CDMS bound by a factor of ~ 3 . Thus, if Nature has picked this corner of the NUHM parameter space, we expect direct detection of dark matter to be imminent. We note that the XENON Collaboration has recently announced a stronger upper limit on the elastic scattering cross section [30]. Consistency with this limit would further require a reduction in the local dark matter density (to its lower limit). Intriguingly, the XENON10 experiment has seen some potential signal events that are, however, interpreted as background. In the following we will show the limits obtained by CDMS, but the potentially somewhat stronger limits from XENON10 should be kept in mind.

This example was for the particular values $\mu = 370$ GeV and $A_0 = -1800$ GeV. We now investigate what happens if these values are varied. Panel a) of Fig. 2 explores the (μ, A_0) plane for $(m_{1/2}, m_0) = (600, 800)$ GeV, values close to the lower tip of the allowed wedge in Fig. 1(a). In this case, the region allowed by the $\text{BR}(B_s \rightarrow \mu^+ \mu^-)$ constraint is *below* the upper dash-dotted black line, and the LEP M_h constraint is satisfied only *above* the dash-dotted red line. We see that only a restricted range $360 \text{ GeV} < \mu < 390 \text{ GeV}$ is compatible with the dark matter constraint. This corresponds to the transition strip where the neutralino is the appropriate bino/Higgsino combination. To the left of this strip, the relic density is too small and to the right, it is too large. Only a very restricted range of $A_0 \sim -1600$ GeV is compatible simultaneously with the M_h and $\text{BR}(B_s \rightarrow \mu^+ \mu^-)$ constraints. Very large negative values of A_0 are excluded as the LSP is the lighter stau. On the (μ, A_0) plane, the elastic scattering cross section is a rapidly decreasing function of μ and is almost independent of A_0 . Indeed, NUHM points excluded by CDMS (or XENON10) generally have low values of μ and M_A [26]. Values of $\mu > 355$ GeV are compatible with CDMS if the strangeness contribution to the proton mass is negligible. For this choice of parameters, the entire displayed plane is compatible with $\text{BR}(b \rightarrow s\gamma)$ and $(g - 2)_\mu$.

Panel b) of Fig. 2 shows what happens if $m_{1/2}$ is increased to 700 GeV, keeping m_0 and the other inputs the same. Compared to Fig. 2(a), we see that the WMAP strip becomes narrower and shifts to larger $\mu \sim 400$ GeV, and that $\text{BR}(b \rightarrow s\gamma)$ starts to exclude a region visible at smaller μ . If $m_{1/2}$ were to be increased much further, the dark matter constraint and $\text{BR}(b \rightarrow s\gamma)$ would no longer be compatible for this value of m_0 . We also

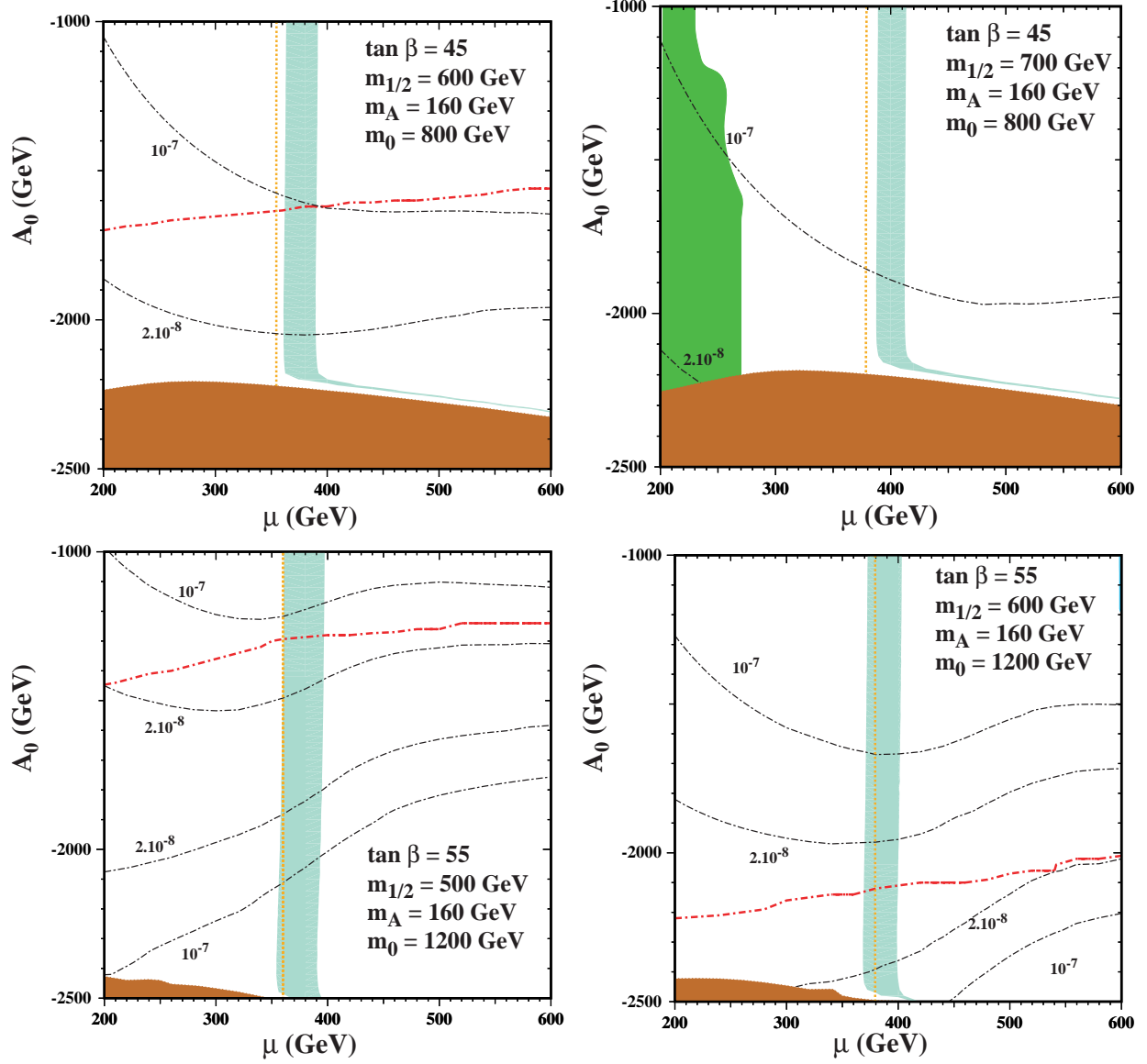


Figure 2: The NUHM parameter space as a function of μ and A_0 for $m_{1/2} = 600(700)$ GeV and $m_0 = 800$ GeV in the left (right) plots. We fix $M_A = 160$ GeV, $\tan \beta = 45(55)$, $m_t = 171.4$ GeV and $m_b = 4.25$ GeV in the upper (lower) plots. For the description of the various lines and shaded areas, see the text.

see that, by comparison with Fig. 2(a), the $\text{BR}(B_s \rightarrow \mu^+\mu^-)$ constraint has moved to lower A_0 , but the M_h constraint has dropped even further, and $M_h > 114$ GeV over the entire visible plane. The net result is a region compatible with all the constraints that extends from $A_0 \sim -1850$ GeV down to $A_0 \sim -2150$ GeV for $\mu \sim 400$ GeV, with a coannihilation filament extending to larger μ when $A_0 \sim -2200$ GeV. Once again all of the WMAP strip in this panel is compatible with CDMS.

The larger allowed area of parameter space is reflected in panel b) of Fig. 1, which has $\mu = 400$ GeV and $A_0 = -2000$ GeV, as well as $\tan\beta = 45$ and $M_A = 160$ GeV as before. In this case, we see that a substantial region of the WMAP strip with $m_{1/2} \sim 700$ GeV and a width $\delta m_{1/2} \sim 100$ GeV, extending from $m_0 \sim 750$ GeV to higher m_0 is allowed by all the other constraints. The $\text{BR}(B_s \rightarrow \mu^+\mu^-)$ and M_h constraints have now moved to relatively low values of $m_{1/2}$, but we still find $\text{BR}(B_s \rightarrow \mu^+\mu^-) > 2 \times 10^{-8}$ and M_h close to the LEP lower limit. We note that the $(g-2)_\mu$ and $\text{BR}(b \rightarrow s\gamma)$ constraints now disfavour a bigger fraction of the parameter space with large $m_{1/2}$, but their only effect here is that $(g-2)_\mu$ truncates the allowed region at $m_0 \sim 1050$ GeV. Once again, the allowed region is compatible with CDMS (to the left of the (orange) dotted line) provided the strangeness contribution to the proton mass is small.

Panels c) and d) of Fig. 1 show the constraints on the $(m_{1/2}, m_0)$ plane for $\tan\beta = 55$ for the same set of input parameters used in panels a) and b). The dominant effects at higher $\tan\beta$ are the shift to the left of the contours of $\text{BR}(B_s \rightarrow \mu^+\mu^-)$ and the exclusion of a much larger portion of the plane at low m_0 due to a stau LSP. Because of the strong dependence on $\tan\beta$, the $\text{BR}(B_s \rightarrow \mu^+\mu^-)$ constraint essentially excludes all values of $m_{1/2} \gtrsim 700$ GeV in panel c) and $\gtrsim 750$ GeV in panel d). Nevertheless, a viable portion of parameter space remains in tact at lower $m_{1/2}$ and higher m_0 . At higher $\tan\beta$, the CDMS bound also becomes stronger and restricts $m_{1/2} \lesssim 560$ GeV in panel c) and $\lesssim 700$ GeV in panel d). Thus in panel c), we are forced into a small triangular region centered at $m_{1/2} \sim 530$ GeV and $m_0 \sim 1350$ GeV bounded by CDMS, M_h , and $(g-2)_\mu$. There, the branching ratio, $\text{BR}(B_s \rightarrow \mu^+\mu^-)$ is near its minimum value of 2×10^{-9} due to the strong cancellation discussed above. In panel d) we are left with a significantly larger quadrilateral region.

The analogous (μ, A_0) planes are shown in Fig. 2c) and d). In panel c), only a small portion of the WMAP strip around $A_0 \sim -1200$ GeV is compatible with both $\text{BR}(B_s \rightarrow \mu^+\mu^-)$ and M_h , while the range in panel d) is considerably larger. In both cases, the CDMS limit is stronger and begins to cut into the WMAP strip.

We have surveyed systematically the allowed region of parameters in the $(m_{1/2}, m_0)$ plane for $\tan\beta$ between 45 and 55, varying the inputs μ and A_0 . To summarize the regions in

the NUHM parameter space which are compatible with CDM and all phenomenological constraints *and* a light heavy Higgs, we first recall that the values of $m_{1/2}$ compatible with WMAP depend on μ , but depend less on m_0 . Specifically, as μ increases, the preferred region of the $(m_{1/2}, m_0)$ plane is a near-vertical strip that moves to larger $m_{1/2}$, which is truncated at low m_0 just above the region where the lighter stau is the LSP. For $\mu < 350$ GeV, there is no WMAP-compliant region compatible with the LEP lower limit on M_h , but a small allowed region appears for μ slightly below 370 GeV. Typical values for $m_{1/2}$ are 500 – 600 GeV at this value of μ and A_0 must be below -1300 GeV. When $\mu = 400$ GeV, the WMAP-compatible strip moves to larger $m_{1/2}$, and there are allowed regions of the $(m_{1/2}, m_0)$ plane for $A_0 \sim -1600$ GeV to ~ -2400 GeV. As μ increases further, the WMAP-compatible strip moves to even larger $m_{1/2}$, and the only allowed region is a small piece of coannihilation strip close to the boundary with the stau LSP region. This region is negligible for $\mu > 500$ GeV. Combining all the allowed values of μ and A_0 , we find that only a small portion of the $(m_{1/2}, m_0)$ plane can ever be compatible with all the constraints. It is roughly triangular in shape, with vertices $(m_{1/2}, m_0) = (500, 1400), (700, 700)$ and $(800, 900)$ GeV.

We now analyse the dependence of the results on the assumption of scalar-mass universality. The assumptions that all squarks with the same electroweak quantum numbers have identical input soft supersymmetry-breaking scalar masses is motivated in general by the suppression of flavour-changing neutral interactions. Specifically, the upper limit on $\text{BR}(B_s \rightarrow \mu^+ \mu^-)$ and the agreement of $\text{BR}(b \rightarrow s \gamma)$ with the SM would require a certain degree of fine-tuning in the presence of large squark mass non-universality. On the other hand, the relative locations of both the WMAP strip and the $(g - 2)_\mu$ constraint depend on the relationship between the soft SUSY-breaking squark and slepton scalar masses. If the slepton masses are *decreased* relative to the squark masses (which we continue to denote by m_0), the lower ends of the WMAP strips in Fig. 1 will *rise* (due to relatively lighter taus), as will the $(g - 2)_\mu$ contours, *raising* the preferred range of m_0 . Conversely, if the slepton masses are *increased* relative to the squark masses, the preferred range of m_0 will be *lower*. Thus, neglecting the universality between squark and slepton masses in general enlarges the allowed region of parameter space that is compatible with the experimental constraints.

We now discuss the possible phenomenological signatures of a scenario with $M_A = 160$ GeV and $\tan \beta \gtrsim 45$ within the NUHM. The interplay of the various constraints in Fig. 1 implies:

- (i) The predicted value of $\text{BR}(B_s \rightarrow \mu^+ \mu^-)$ in the allowed region is generally $> 2 \times 10^{-8}$. Thus, this channel may offer good prospects within the near future for either supporting or contradicting the NUHM interpretation of the weaker CDF $\tan \beta$ bound,

as compared to the expected sensitivity.

- (ii) We find that M_h must be very close to the LEP lower limit, i.e. in the range where LEP observed a couple of Higgs-like events [15]. This part of parameter space could be probed at the Tevatron with 8 fb^{-1} of integrated luminosity. Due to the large value of $\tan \beta$ and the small mass of the A boson, the rates of h decays into bottom quarks and tau leptons are enhanced as compared to the SM.
- (iii) The predicted value of $\text{BR}(b \rightarrow s\gamma)$ in the allowed region is $\sim 4.6 \times 10^{-4}$, which is about one σ above the current experimental value (if the experimental and theory errors are added linearly). Consequently, an improvement in the present theoretical uncertainty might enable a discrepancy to appear between $\text{BR}(b \rightarrow s\gamma)$ and the SM value.
- (iv) The discrepancy between the experimental measurement of $(g-2)_\mu$ and the SM calculation can easily be explained in this scenario, although the $(g-2)_\mu$ discrepancy should be somewhat smaller than the current central value. However, a much smaller discrepancy (corresponding to larger m_0 values) could also be accommodated.
- (v) Confronting the prediction for $\text{BR}(B_u \rightarrow \tau\nu_\tau)$ [31] with the measurement from Belle and BABAR [32] already yields interesting constraints on the charged Higgs-boson mass as a function of $\tan \beta$, although the present experimental errors are still very large, see e.g. Ref. [33]. In the scenario considered here $\text{BR}(B_u \rightarrow \tau\nu_\tau)$ is predicted to be relatively low as compared to its SM value, where the ratio of MSSM/SM is ~ 0.33 . This is about one σ below the current central value.
- (vi) The ratio of the B_s mass difference to the SM prediction is close to unity, ~ 0.91 [31]. In view of the theoretical uncertainties, it will be difficult to establish such a small deviation.
- (vii) The W boson mass is predicted to be [34, 35] relatively low, $M_W \sim 80.367 \text{ GeV}$, i.e. again about one σ below the current central experimental value.
- (viii) The masses of the other SUSY particles are estimated to be $m_{\tilde{\chi}_1^0} \sim 210\text{--}270 \text{ GeV}$, $m_{\tilde{\tau}_1} \sim 310\text{--}800 \text{ GeV}$, $m_{\tilde{\chi}_1^\pm}, m_{\tilde{\chi}_2^0} \sim 340\text{--}390 \text{ GeV}$, $m_{\tilde{\chi}_3^0} \sim 370\text{--}410 \text{ GeV}$, $m_{\tilde{\chi}_2^\pm}, m_{\tilde{\chi}_4^0} \sim 480\text{--}590 \text{ GeV}$, $m_{\tilde{\tau}_2}, m_{\tilde{\nu}_\tau} \sim 770\text{--}1120 \text{ GeV}$, $m_{\tilde{e}_R} \sim 870\text{--}1250 \text{ GeV}$, $m_{\tilde{e}_L}, m_{\tilde{\nu}_e} \sim 960\text{--}1310 \text{ GeV}$, $m_{\tilde{g}} \sim 1270\text{--}1570 \text{ GeV}$, and for the squarks $m_{\tilde{t}_1} \sim 1250 \text{ GeV}$, $m_{\tilde{t}_2}, m_{\tilde{b}_1} \sim 1450 \text{ GeV}$, $m_{\tilde{b}_2} \sim 1550 \text{ GeV}$, $m_{\tilde{u}_{L,R}}, m_{\tilde{d}_{L,R}} \sim 1600 \text{ GeV}$, each with uncertainties \sim

10%. The sparticle spectrum is not particularly light, and at the Tevatron no further SUSY particle discoveries could be expected. On the other hand, the strongly-interacting sparticles should mostly be within reach of the LHC, and many weakly-interacting sparticles should be visible in their cascade decays. At the ILC, depending on the center-of-mass energy, the lighter neutralinos, charginos and staus could be produced.

- (ix) Direct detection experiments should see a signal at current sensitivities. The lack of a signal in the CDMS experiment could be explained by a reduced strangeness contribution to the proton mass. The reported XENON10 limit would further require a reduction in the local halo density (to its lower limit).

Performing a χ^2 fit for nine precision and B -physics observables along the lines of Ref. [19] yields a total value of $\chi^2_{\text{tot}} \sim 9 - 10$ in the allowed part of the NUHM parameter space, where even slightly smaller values can be found for $M_h \lesssim 114$ GeV.⁶

Very likely the weaker CDF $\tan \beta$ bound from the search for heavy Higgs bosons compared to its expected sensitivity is due to a statistical fluctuation that will eventually evaporate. Nevertheless, it is interesting to know whether a signal at this level could be accommodated within the MSSM. We have shown that $M_A \sim 160$ GeV is possible for $\tan \beta \gtrsim 45$ within the NUHM, though it stretches various experimental constraints to their limits. Correspondingly, small improvements in some of these measurements, e.g., of $\text{BR}(B_s \rightarrow \mu^+ \mu^-)$ or of the dark matter scattering rate, would either exclude such a signal in the NUHM framework, or else provide supporting evidence. One way or another, it should be possible soon to cast light on the interpretation of the CDF search.

Acknowledgements

We would like to thank Patricia Ball, Prisca Cushman, and Athanasios Dedes for useful conversations. The work of K.A.O. was partially supported by DOE grant DE-FG02-94ER-40823. The work of S.H. was partially supported by CICYT (grant FPA2006-02315). Work supported in part by the European Community's Marie-Curie Research Training Network under contract MRTN-CT-2006-035505 'Tools and Precision Calculations for Physics Discoveries at Colliders'.

⁶It should be kept in mind that the $M_h = 114$ GeV lines shown in the plots are roughly the LEP 95% C.L. exclusion limits, not the 2σ bound. In applying this bound the current theory uncertainty in the M_h prediction of ~ 3 GeV needs to be taken into account.

References

- [1] A. Abulencia et al. [CDF Collaboration], *Phys. Rev. Lett.* **96** (2006) 011802, hep-ex/0508051.
- [2] V. Abazov et al. [D0 Collaboration], *Phys. Rev. Lett.* **97** (2006) 121802, hep-ex/0605009.
- [3] A. Abulencia et al. [CDF Collaboration], *Phys. Rev. Lett.* **96** (2006) 042003, hep-ex/0510065.
- [4] CDF Collaboration, CDF note 8676, see:
http://www-cdf.fnal.gov/~aa/mssm_htt_1fb/note/cdf8676.pdf.
- [5] D0 Collaboration, D0 Note 5331-CONF, see:
<http://www-d0.fnal.gov/cgi-bin/d0note?5331>.
- [6] G. Landsberg, talk given at *Rencontres de Moriond: QCD and Hadronic interactions*, La Thuile (Italy), March 17-24 2007, see:
<http://moriond.in2p3.fr/QCD/2007/WednesdayMorning/Landsberg.pdf> (p. 20).
- [7] M. Carena, S. Heinemeyer, C. Wagner and G. Weiglein, *Eur. Phys. J. C* **45** (2006) 797, hep-ph/0511023.
- [8] D. Spergel et al. [WMAP Collaboration], astro-ph/0603449.
- [9] J. Ellis, K. Olive and Y. Santoso, *Phys. Lett. B* **539** (2002) 107, hep-ph/0204192.
- [10] J. Ellis, T. Falk, K. Olive and Y. Santoso, *Nucl. Phys. B* **652** (2003) 259, hep-ph/0210205.
- [11] M. Olechowski and S. Pokorski, *Phys. Lett. B* **344** (1995) 201, hep-ph/9407404; V. Berezhinsky, A. Bottino, J. Ellis, N. Fornengo, G. Mignola and S. Scopel, *Astropart. Phys.* **5** (1996) 1, hep-ph/9508249; M. Drees, M. Nojiri, D. Roy and Y. Yamada, *Phys. Rev. D* **56** (1997) 276, [Erratum-ibid. **D 64** (1997) 039901], hep-ph/9701219; M. Drees, Y. Kim, M. Nojiri, D. Toya, K. Hasuko and T. Kobayashi, *Phys. Rev. D* **63** (2001) 035008, hep-ph/0007202; P. Nath and R. Arnowitt, *Phys. Rev. D* **56** (1997) 2820, hep-ph/9701301; J. Ellis, T. Falk, G. Ganis, K. Olive and M. Schmitt, *Phys. Rev. D* **58** (1998) 095002, hep-ph/9801445; J. Ellis, T. Falk, G. Ganis and K. Olive, *Phys. Rev. D* **62** (2000) 075010, hep-ph/0004169; A. Bottino, F. Donato, N. Fornengo and S. Scopel, *Phys. Rev. D* **63** (2001) 125003, hep-ph/0010203; S. Profumo, *Phys. Rev. D*

- 68** (2003) 015006, hep-ph/0304071; D. Cerdeno and C. Munoz, *JHEP* **0410** (2004) 015, hep-ph/0405057; H. Baer, A. Mustafayev, S. Profumo, A. Belyaev and X. Tata, *JHEP* **0507** (2005) 065, hep-ph/0504001.
- [12] E. Barberio et al. [Heavy Flavor Averaging Group (HFAG)], hep-ex/0603003, see: <http://www.slac.stanford.edu/xorg/hfag/>.
- [13] J. Ellis, S. Heinemeyer, K. Olive and G. Weiglein, *JHEP* **0605** (2006) 005, hep-ph/0602220.
- [14] LEP Higgs working group, *Phys. Lett. B* **565** (2003) 61, hep-ex/0306033.
- [15] LEP Higgs working group, *Eur. Phys. J. C* **47** (2006) 547, hep-ex/0602042.
- [16] CDF Collaboration, CDF Public Note 8176, see: <http://www-cdf.fnal.gov/physics/new/bottom/060316.blessed-bsmumu3/> .
- [17] D0 Collaboration, D0 Note 5344-Conf, see: <http://www-d0.fnal.gov/Run2Physics/WWW/results/b.htm> .
- [18] H. Goldberg, *Phys. Rev. Lett.* **50** (1983) 1419; J. Ellis, J. Hagelin, D. Nanopoulos, K. Olive and M. Srednicki, *Nucl. Phys. B* **238** (1984) 453.
- [19] J. Ellis, S. Heinemeyer, K. Olive, A.M. Weber and G. Weiglein, arXiv:0706.0652 [hep-ph].
- [20] M. Misiak et al., *Phys. Rev. Lett.* **98** (2007) 022002, hep-ph/0609232.
- [21] P. Gambino and M. Misiak, *Nucl. Phys. B* **611** (2001) 338, hep-ph/0104034.
- [22] J. Ellis, K. Olive and V. Spanos, *Phys. Lett. B* **624** (2005) 47, hep-ph/0504196. J. Ellis, K. Olive, Y. Santoso and V. Spanos, *JHEP* **0605** (2006) 063, hep-ph/0603136.
- [23] M. Davier, hep-ph/0701163.
- [24] S. Heinemeyer, W. Hollik and G. Weiglein, *Comp. Phys. Commun.* **124** 2000 76, hep-ph/9812320; *Eur. Phys. J. C* **9** (1999) 343, hep-ph/9812472; G. Degrandi, S. Heinemeyer, W. Hollik, P. Slavich and G. Weiglein, *Eur. Phys. J. C* **28** (2003) 133, hep-ph/0212020; M. Frank, T. Hahn, S. Heinemeyer, W. Hollik, H. Rzehak and G. Weiglein, *JHEP* **02** (2007) 047, hep-ph/0611326; the code is available via <http://www.feynhiggs.de> .

- [25] D0 Collaboration, D0 Note 5344-Conf, see:
<http://www-d0.fnal.gov/Run2Physics/WWW/results/b.htm> .
- [26] J. Ellis, K. Olive, Y. Santoso and V. Spanos, *Phys. Rev. D* **71** (2005) 095007, hep-ph/0502001.
- [27] M. Carena, D. Hooper and P. Skands, *Phys. Rev. Lett.* **97** (2006) 051801, hep-ph/0603180.
- [28] J. Gasser, H. Leutwyler and M. Sainio, *Phys. Lett. B* **253** (1991) 252; M. Knecht, hep-ph/9912443; M. Sainio, *PiN Newslett.* **16** (2002) 138, hep-ph/0110413.
- [29] D. Akerib et al. [CDMS Collaboration], *Phys. Rev. Lett.* **96** (2006) 011302, astro-ph/0509259.
- [30] J. Angle et al. [XENON Collaboration], arXiv:0706.0039 [astro-ph],
 see also: <http://xenon.astro.columbia.edu/> .
- [31] G. Isidori and P. Paradisi, *Phys. Lett. B* **639** (2006) 499, hep-ph/0605012.
- [32] K. Ikado et al. [Belle Collaboration], hep-ex/0604018; B. Aubert et al. [BABAR Collaboration], arXiv:0705.1820 [hep-ex].
- [33] S. Villa, talk given at *FPCP07, 5th Flavor Physics and CP Violation Conference*, Bled (Slovenia), May 12–16 2007, see: <http://www-f9.ijs.si/fpcp07>.
- [34] S. Heinemeyer, W. Hollik, D. Stöckinger, A.M. Weber and G. Weiglein, *JHEP* **08** (2006) 052, hep-ph/0604147.
- [35] S. Heinemeyer, W. Hollik and G. Weiglein, *Phys. Rept.* **425** (2006) 265, hep-ph/0412214.